nature COMMUNICATIONS

OPEN

ARTICLE

Received 7 Sep 2011 | Accepted 31 Jan 2012 | Published 20 Mar 2012

DOI: 10.1038/ncomms1716

Rice APC/C^{TE} controls tillering by mediating the degradation of MONOCULM 1

Qibing Lin[1,*], Dan Wang[1,*], Hui Dong[2,*], Suhai Gu[1], Zhijun Cheng[1], Jie Gong[2], Ruizhen Qin[1], Ling Jiang[2], Gang Li[3], Jiu Lin Wang[1], Fuqing Wu[1], Xiuping Guo[1], Xin Zhang[1], Cailin Lei[1], Haiyang Wang[1] & Jianmin Wan[1,2]

Rice *MONOCULM 1* (*MOC1*) and its orthologues *LS/LAS* (lateral suppressor in tomato and *Arabidopsis*) are key promoting factors of shoot branching and tillering in higher plants. However, the molecular mechanisms regulating MOC1/LS/LAS have remained elusive. Here we show that the rice *tiller enhancer* (*te*) mutant displays a drastically increased tiller number. We demonstrate that *TE* encodes a rice homologue of Cdh1, and that *TE* acts as an activator of the anaphase promoting complex/cyclosome (APC/C) complex. We show that *TE* coexpresses with *MOC1* in the axil of leaves, where the APC/C^{TE} complex mediates the degradation of MOC1 by the ubiquitin–26S proteasome pathway, and consequently downregulates the expression of the meristem identity gene *Oryza sativa homeobox 1*, thus repressing axillary meristem initiation and formation. We conclude that besides having a conserved role in regulating cell cycle, APC/C^{TE} has a unique function in regulating the plant-specific postembryonic shoot branching and tillering, which are major determinants of plant architecture and grain yield.

[1] National Key Facility for Crop Gene Resources and Genetic Improvement, Institute of Crop Science, Chinese Academy of Agricultural Sciences, Beijing 100081, China. [2] National Key Laboratory for Crop Genetics and Germplasm Enhancement, Jiangsu Plant Gene Engineering Research Center, Nanjing Agricultural University, Nanjing 210095, China. [3] Department of Molecular, Cellular, and Developmental Biology, Yale University, New Haven, Connecticut 06520-8104, USA. *These authors contributed equally to this work. Correspondence and requests for materials should be addressed to J.W. (email: wanjm@caas.net.cn).

Targeted protein degradation through the ubiquitin–proteasome system is a major regulatory mechanism of cell-cycle progression. Cdh1 (also known as Hct1 in budding yeast, Ste9 or Srw1 in fission yeast, Fzr in human and CCS52 in plants) is a substrate-recognition and -binding factor of the multimeric APC/C E3 ubiquitin ligase[1]. It is thought that Cdh1 activates APC/C in late mitosis and during G0/G1 by targeted degradation of key cell-cycle regulators (such as cyclins or inhibitors of cyclin-dependent kinases) by the 26S proteasome to promote mitotic exit, maintain G0/G1 phase and regulate the endocycle in animals[1–7]. Studies in *Arabidopsis thaliana*, legumes and tomato have also demonstrated that APC/C^{CCS52} regulates cell division, cell expansion, endocycle and root meristem maintenance[3,4,8–12]. However, other than mitotic cyclins, no substrates of APC/C^{CCS52} have been identified yet, and the regulatory mechanisms of APC/C^{CCS52} have remained essentially unknown in plants.

Tillering and branching, the formation of lateral shoots, is an important determinant of plant architecture and crop yield[13,14], and a complex process that is regulated by several genetic pathways[15–21]. The rice gene *MOC1* and its orthologues *LS*/*LAS* encode transcriptional regulators of the GRAS family and are key promoting factors of tillering and branching in both monocot and dicot species[15–17]. Previous studies have shown that the *LAS* and *MOC1* act upstream of *SHOOT-MERISTEMLESS* (*STM*) in *Arabidopsis* and *OSH1* (the homologue of *Knotted-1* in maize) during the initiation and establishment of AM[16,17,22–24]. However, the regulatory mechanisms of MOC1/LS/LAS have remained elusive.

Here we report the identification of a *tiller enhancer* (*te*) mutant with many more tillers than wild-type rice. We show that *TE* is a rice homologue of *Cdh1*, and it acts as an activator of APC/C to control rice tillering by mediating the degradation of MOC1 protein and, subsequently, reducing the expression of the meristem identity gene *OSH1*. Our results provide new insights into the function and regulatory mechanisms of APC/C$^{TE(Cdh1)}$ E3 ligases in higher plants.

Results

The *te* mutant displays the pleiotropic phenotypes. Rice-plant architecture is crucial for grain yield and is determined by tiller number and angle, plant height, panicle morphology, leaf structure and root systems[13,25]. To identify new regulators of rice architecture, we isolated the rice *te* mutant from a mutant pool[26]. *te* had a similar number of tillers as wild-type (WT) plants till the seventh leaf stage (Fig. 1a). However, by the heading stage, the total tiller number of *te* was about 3-fold that of WT, resulting from additional tillers produced on both low nodes and high nodes (Fig. 1b–d). In addition to increased tillers, the *te* mutant shows a dwarf phenotype with much shorter internodes II–V (Fig. 1e,f). Microscopy observation revealed that the shortening of *te* stem was mainly due to a reduction in cell number, as the cell sizes in internodes were largely comparable between WT and *te* (Fig. 1g,h). Moreover, the *te* mutant also displays a twisted flag leaf and panicle phenotype (Fig. 1i–k).

***TE* encodes a rice homologue of Cdh1**. We used a map-based approach to place the *TE* locus within a 23-kb DNA region on the BAC098695 clone of chromosome 3, which contains four predicted genes. Two mutations, a deletion of nucleotide 38 (C) and a substitution of nucleotide 40 (C–G) downstream of the ATG initiation codon, were identified in the first exon of one of the predicted genes (LOC_Os03g03150) (Fig. 1l). These mutations result in a frameshift and a 216-amino acid truncated protein product (Supplementary Fig. S1). Genetic complementation showed that a genomic fragment containing the wild-type DNA (pGTE) completely rescued the *te* mutant phenotypes (Fig. 1m). We thus concluded that LOC_Os03g03150 corresponds to the *TE* gene. Sequence and phylogenetic analyses revealed that *TE* encodes a rice homologue of Cdh1 class proteins with a conserved WD-40 repeats domain and four motifs (C-box, CSM, RVL and IR) commonly found in other Cdh1 homologues (Supplementary Figs S1 and S2).

Quantitative reverse transcriptase–PCR analysis revealed that *TE* is widely expressed in roots, shoots, leaves and panicles (Fig. 2a). RNA *in situ* hybridization analysis demonstrated that *TE* is primarily expressed in the AM in axils from P1 to P5 leaf stage, shoot apical meristem and root meristem, and actively proliferative tissues such as young leaves (Fig. 2b–e). Thus, the expression pattern of *TE* is consistent with the phenotypes of *te* mutant.

As reported for other Cdh1 homologues such as AtCCS52A1 and AtCCS52A2[8], transient expression analysis in *Arabidopsis* protoplasts revealed that the TE–GFP fusion protein is predominantly targeted to the nucleus (Fig. 2f). Overexpression of *TE* in *Schizosaccharomyces pombe* inhibited cell division and caused cell enlargement (Fig. 3a,b). Consistent with this observation, flow cytometry and 4′,6-diamidino-2-phenylindole staining analyses showed that some cells in the *te* flag leaves had 4C DNA content and were binucleated compared with WT, suggesting a delay in mitotic exit in some *te* leaf cells (Fig. 3c–f). Notably, more binucleated cells have been observed in mice *Fzr1*$^{-/-}$ mouse embryonic fibroblasts (*Cdh1*-deficient cells) because of delayed mitotic exit[27]. Taken together, these results support the notion that *TE* has an evolutionarily conserved role in cell-cycle regulation[2,27,28].

TE physically interacts with MOC1 and OsCDC27. It has been reported previously that Cdh1 mainly recognizes the D-box (RxxLxxxxN/D/E) and KEN-box in the amino-terminal region of its substrates to target them for ubiquitination and degradation by the 26S proteasome[1,7]. The enhanced tillering phenotype in the *loss-of-function te* mutant suggests that TE could participate in targeted degradation of a positive regulator(s) of tillering. Through extensive analysis of known positive regulators of tillering and branching, we identified a typical D-box in the N-terminal region of the MOC1/LS/LAS protein (Supplementary Fig. S3a). Previous studies have reported a *loss-of-function moc1* mutant that has dramatically reduced tiller number, whereas *MOC1*-overexpressing lines have increased tiller number[17]. Thus, we tested whether TE physically interacts with MOC1. A yeast two-hybrid assay showed that TE interacted with MOC1, but not with MOC1-d (deletion of 107 amino acids in the N-terminal region) or MOC1-m (in which the typical D-box was mutated) (Fig. 4a). In addition, an *in vitro* pull-down assay showed that MBP–TE protein but not the MBP control pulled down MOC1 protein from the total protein extracts of WT rice plants (Fig. 4b). Moreover, biomolecular fluorescence complementation (BiFC) assay showed that TE interacted with MOC1 in *Nicotiana benthamiana* leaf cells (Fig. 4c). These results suggest that TE directly interacts with MOC1 and that the D-box in the N-terminal region of MOC1 is required for its physical interaction with TE.

Cdh1 activates the activity of APC/C^{Cdh1} E3 ubiquitin ligase by coupling to the CDC27 subunit of the APC/C complex[1,7]. The rice genome contains a single *CDC27* gene, *OsCDC27* (Supplementary Fig. S3b,c). We confirmed that TE indeed physically interacts with OsCDC27 using yeast two-hybrid, *in vitro* pull-down and BiFC assays (Fig. 4a–c). These results support the notion that TE acts as an activator of APC/C E3 ubiquitin ligase by directly coupling to the OsCDC27 subunit of the APC/C complex.

TE mediates the degradation of MOC1. We next conducted a series of biochemical experiments to test whether TE mediates the proteolysis of MOC1. An *in vitro* ubiquitination assay showed that MOC1 was polyubiquitinated by the total protein extracts of WT plants, but not by extracts of *te* plants (Fig. 5a, Supplementary Fig. S4), indicating that TE is required for MOC1's ubiquitination. In addition, a cell-free degradation study showed that purified recombinant MBP–MOC1 protein, but not the MBP–MOC1-m protein

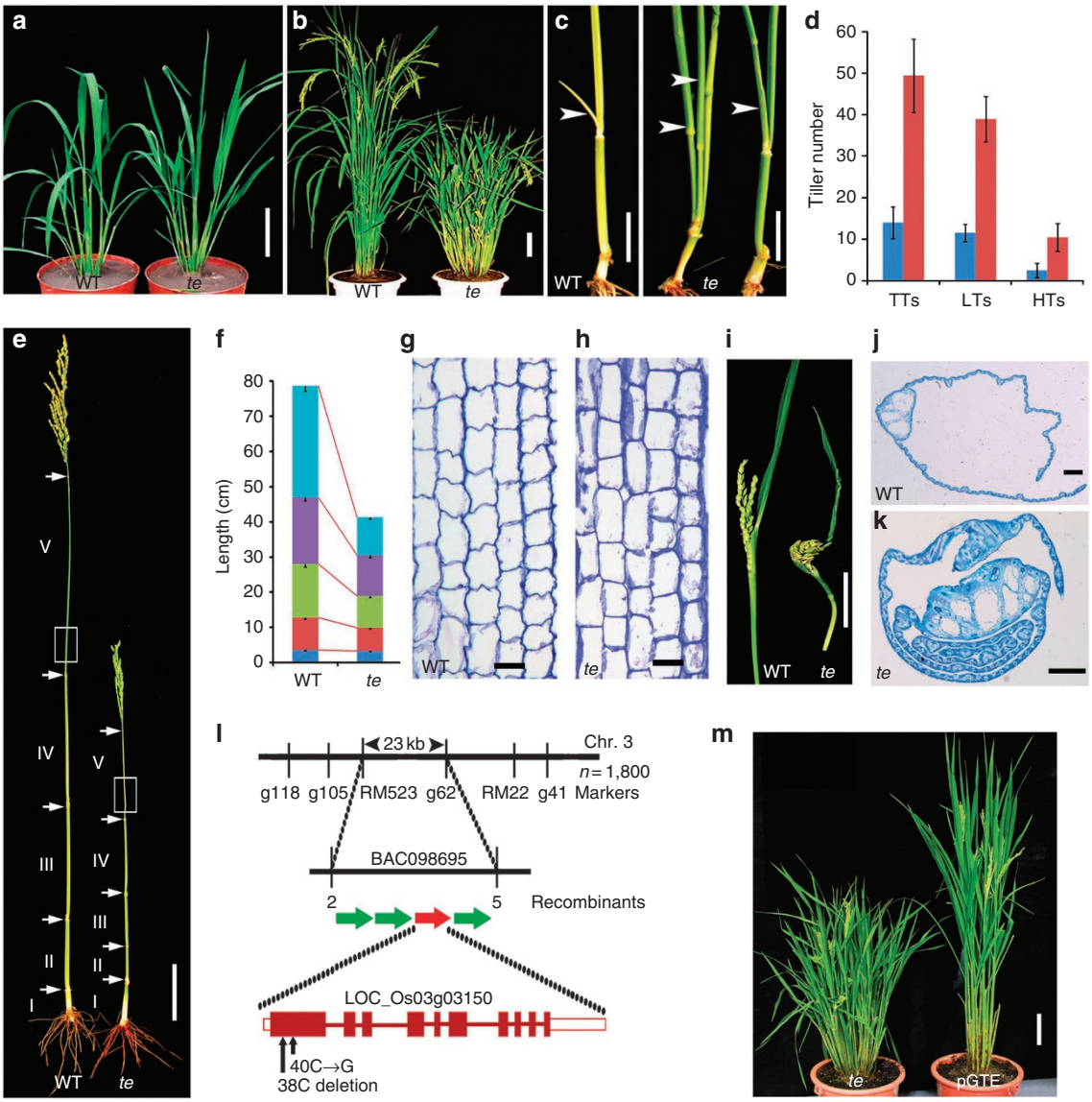

Figure 1 | Phenotype characterization of *te* mutant and map-based cloning of *TE*. (**a**) Phenotype of WT and *te* plants at the seventh leaf stage. (**b**) Phenotype of WT and *te* plants at the heading stage. (**c**) WT produces un-elongated lateral bud (left panel, arrowhead) on the elongated upper internodes, whereas *te* mutant produces additional tillers (right panel, arrowhead) from the elongated internodes. (**d**) Tiller number comparison between WT (blue) and *te* (red) plants at the heading stage. TTs, total tillers; LTs, lower node tillers; HTs, higher node tillers. LTs are the tillers outgrown from the un-elongated basal internodes. HTs are the tillers outgrown from the elongated internodes. (**e**) Stem structure of WT and *te*. (**f**) Internode length comparison between WT and *te*. I (light blue), II (purple), III (green), IV (red) and V (blue) indicate the first, the second, the third, fourth and fifth internode, respectively. (**g**,**h**) Longitudinal sections of the corresponding parts of the fifth internode (V) between WT (**g**) and *te* (**h**) (marked by white boxes in **e**). Scale bar, 50 μm. (**i**) The twisted panicle and flag leaf phenotype of *te* mutant. (**j**,**k**) Cross section images of flag leaf of WT (**j**) and *te* mutant (**k**) showing the highly twisted flag leaf structure of *te* mutant. (**l**) Mapping of *TE* locus (LOC_Os03g03150) and the molecular lesions in the *te* mutant. (**m**) pGTE rescued the *te* mutant phenotype. Data are mean ± s.d. ($n = 30$ plants) in **d**,**f**. (**a**,**b**,**c**,**e**,**i**,**m**) Scale bar, 10 cm, (**g**,**h**) 50 μm and (**j**,**k**) 500 μm.

and MBP control, was rapidly degraded by the total protein extracts of WT plants, but not by extracts of *te* plants (Fig. 5b). Moreover, MG132, a specific inhibitor of the 26S proteasome, blocked the degradation of MBP–MOC1 in the total protein extracts (Fig. 5b). Further, MOC1 protein level was markedly higher in *te* plants compared with WT plants (Fig. 5c) whereas *TE*-overexpression lines (*TE*-OE) had reduced MOC1 accumulation and reduced tiller number (Fig. 5d–f). Taken together, these results support the view that TE regulates tillering in rice by mediating the degradation of MOC1 by the ubiquitin–26S proteasome pathway.

To further determine the genetic interaction between TE and MOC1, we isolated a new allele of *moc1*, termed *moc1-5*, and constructed the *te moc1-5* double mutant. Map-based cloning and sequence analysis identified a deletion of nucleotide 38 (C) downstream of the ATG initiation codon of the *MOC1* gene (LOC_Os06g40780) in the *moc1-5* mutant (Supplementary Fig. S5a), leading to a frame-shift and a 267-amino acid truncated protein product. Western blot analysis confirmed the absence of the MOC1 protein in *moc1-5* mutant (Supplementary Fig. S5b). Like the *moc1-5* mutant, the *te moc1-5* double mutant had significantly reduced number of tillers (Fig. 5g), suggesting that *MOC1* acts downstream of *TE* in control of tillering. Consistent with this, the expression of *OSH1*[24,29,30] (a key meristem identity gene) and *OsTB1*[31] (a rice homologue of maize *TB1*[32]) was markedly lower in our *TE*-OE

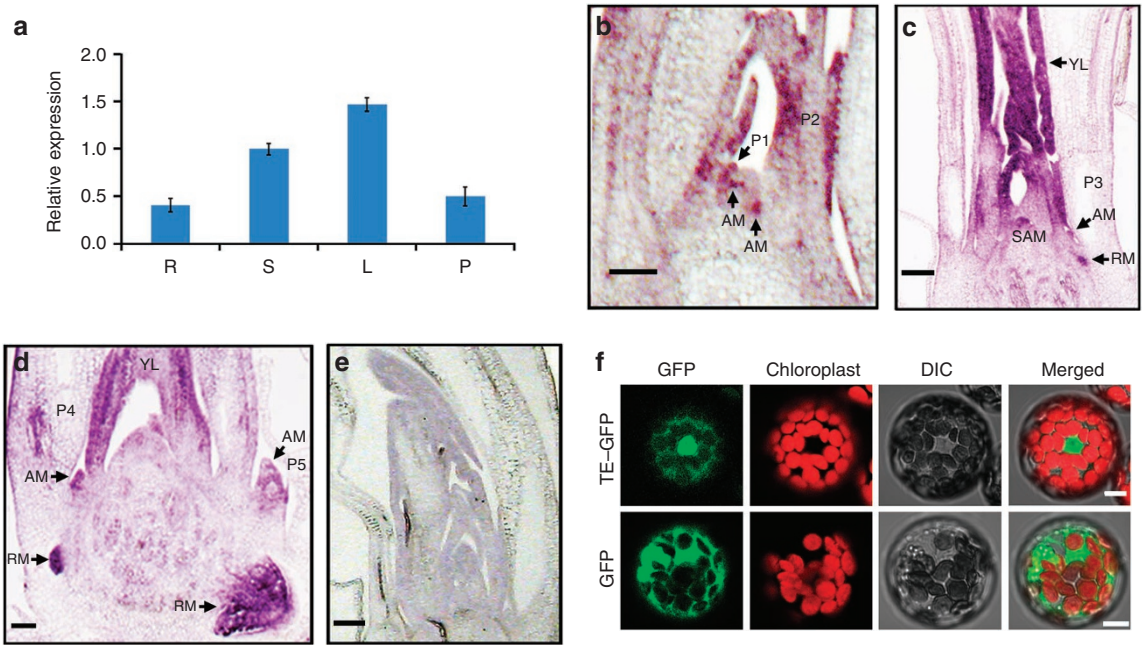

Figure 2 | *TE* expression pattern and subcelluar localization of TE protein. (**a**) Quantitative RT–PCR analysis showing the relative expression levels of *TE* in root (R), shoot (S), leaf (L) and panicle (P). Error bars represent s.e.m. ($n = 3$). (**b**) RNA *in situ* hybridization in longitudinal section showing that *TE* is preferentially expressed in the AM in axils of P1 and P2 leaf, P1 leaf primordia and young leaves (YL) at P2 leaf stage. (**c**) RNA *in situ* hybridization in longitudinal section showing that *TE* is preferentially expressed in the shoot apical meristem (SAM), AM in axils of P3 leaf, root meristem (RM) and YL at P3 leaf stage. (**d**) RNA *in situ* hybridization in longitudinal section showing that *TE* is preferentially expressed in the AM in axils of P4 leaf and P5 leaf, RM and YL at P4 leaf stage. (**e**) The sense probe of *TE* was used as a negative control. (**f**) TE-GFP fusion protein is predominantly localized to the nuclei of *Arabidopsis* protoplasts (upper images); GFP protein itself is distributed throughout the cytoplasm of *Arabidopsis* protoplasts (lower images). (**b**–**e**) Scale bar, 100 μm and (**f**) 7.5 μm.

lines as in *moc1* mutant[17] (Fig. 5h,i), further supporting the notion that TE and MOC1 act in the same genetic pathway in control of tillering.

Discussion

Tillering or formation of shoot branches is a postembryonic developmental process unique to higher plants. The shoot branches originate from AMs that are produced in the axils of the leaves. Several key regulators involved in AM formation have been identified in plants, including REVOLUTA[33], LAS[16] and Regulator of Axillary Meristem[34] in *Arabidopsis*, LS[15,16] and Blind in tomato[35], Barren Stalk1 (BA1)[19] in maize, MOC1[17], Lax Panicle1[18,36] and Lax Panicle2[21] in rice. Here, we have identified a new negative regulator of tillering in rice, TE, and demonstrated that it acts as an activator of APC/C E3 ubiquitin ligase. We further showed that TE has a conserved role in cell-cycle regulation and that it regulates rice tillering by mediating the degradation of MOC1 (Fig. 5j), and consequently downregulates the expression of the meristem identity gene *OSH1* (Fig. 5h), thus repressing AM initiation and formation. These results indicate that plants and animals could use conserved cell-cycle machineries to regulate distinct developmental processes. To our knowledge, MOC1 is the first reported substrate of APC/C^{CCS52} that is not a mitotic cyclins in plants, and its orthologues in tomato (LS) and *Arabidopsis* (LAS) have also been shown to have a similar role in regulating lateral branching (shoot and panicle branching)[15,16]. In addition, the putative orthologues of TE (CCS52 proteins in Arabidopsis, maize, tomato and legume)[4,8,12,37] and OSH1 (KN1 in maize and STM in *Arabidopsis*)[22,23] could be identified in both monocot and dicot species. Further, previous studies have shown that LAS acts upstream of *REVOLUTA*, which is needed to activate the expression of *STM* in *Arabidopsis*[16,33]. These results together suggest that a conserved genetic pathway (TE(CCS52A)–MOC1(LAS)–*OSH1*(*STM*)) likely operates in both monocots and dicots to control tillering and shoot branching. The observed overlap of *TE* and *MOC1* expression in the axil from P2 to P3 leaf stage (Fig. 2b–d, refs 17 and 36) suggests that a link probably exists between the levels of TE and MOC1 proteins to the state of stem cell-like cells in the axils from P1 to P3 leaf stage. We speculate that TE might act to maintain these stem cell-like cells in a mitotically inactive and indeterminate state through targeted proteolysis of MOC1, a key AM-initiation-promoting factor (refs 17 and 36). In further support of this notion, we have demonstrated that *TE*-OE lines have much fewer tillers concomitant with reduced level of MOC1 protein accumulation, whereas the *loss-of-function te* mutants have much more tillers concomitant with the elevated level of MOC1 protein accumulation (Fig. 5).

In addition to cell-cycle regulation, APC/C^{Cdh1} has been reported to have important roles in regulating hematopoiesis, neurogenesis, lens development, myogenesis, genomic stability and tumour suppression by targeted degradation of specific key regulators of these developmental processes in animals[2,28,38]. APC/C^{CCS52} has also been shown to regulate root development in plants[8]. In this study, we found that the *te* mutant displayed a pleiotropic phenotype, including shortened stem and flag leaves, twisted flag leaves and panicles (Fig. 1e–k), suggesting that, as in animals, APC/C^{CCS52A} also has important roles in regulating a variety of developmental processes in plants. Further investigation of the detailed mechanisms of APC/$C^{TE(CCS52A)}$ regulating plant morphogenesis, and the functional relationship of the (TE(CCS52A)-MOC1(LAS)-*OSH1*(*STM*)) pathway with other developmental pathways regulating branching pattern (such as the Lax Panicle1/BA1 pathway[18,19,36] and the MAX/RMS/D pathway[39]), may provide new strategies for genetic improvement of crop architecture to optimize grain yield.

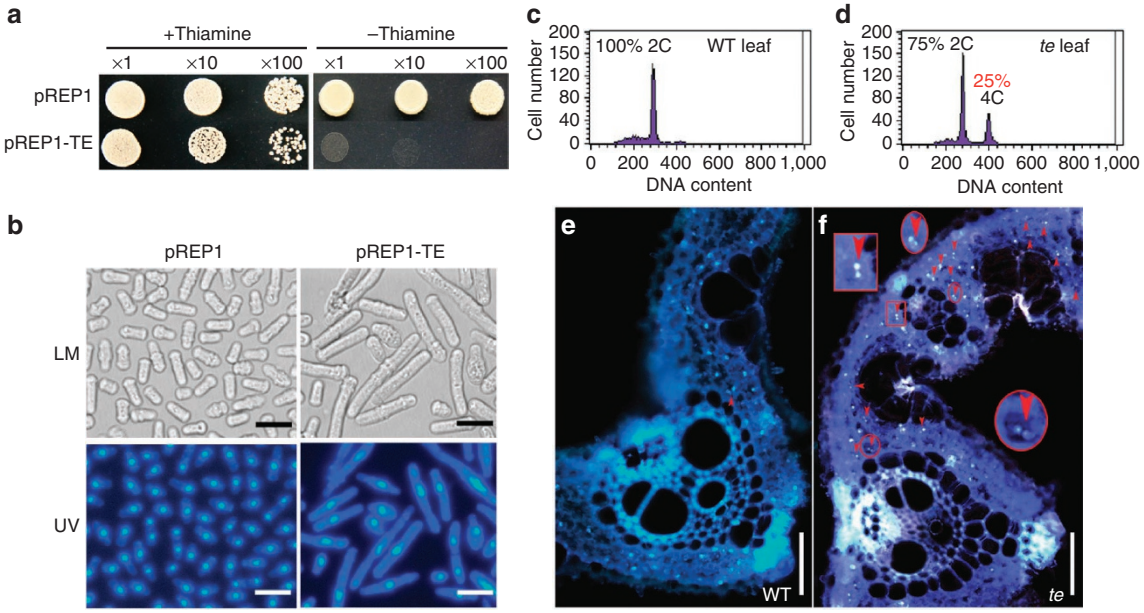

Figure 3 | Conserved role of *TE* in cell-cycle regulation. (**a**) Growth of *S. pombe* transformed with the empty vector pREP1 and pREP1-TE in the presence (+thiamine, the expression of *TE* is repressed in the presence of thiamine) or absence of thiamine (−thiamine, the expression of *TE* is induced in the absence of thiamine). (**b**) The observation of *S. pombe* cells under light microscopy and 4′,6-diamidino-2-phenylindole (DAPI)-stained cells under UV light showing the *S. pombe* cells transformed with pREP1-TE in the absence of thiamine became much larger and longer concomitant with bigger nuclei compared with pREP1. LM, light microscopy; UV, observation of DAPI-stained cells under UV light. (**c**,**d**) Flow cytometry analysis showing that some (about 25%) flag leaf cells of *te* mutant (**d**) have 4C DNA content compared with WT (**c**). (**e**,**f**) Microscopy images of transverse sections (stained with DAPI) showing that the flag leaves of *te* (**f**) have more cells with two nuclei (indicated by arrowheads) compared with WT flag leaves (**e**). The inset magnified parts in **f** showing two nuclei in one cell. (**b**) Scale bar, 10 μm and (**e**,**f**) 50 μm.

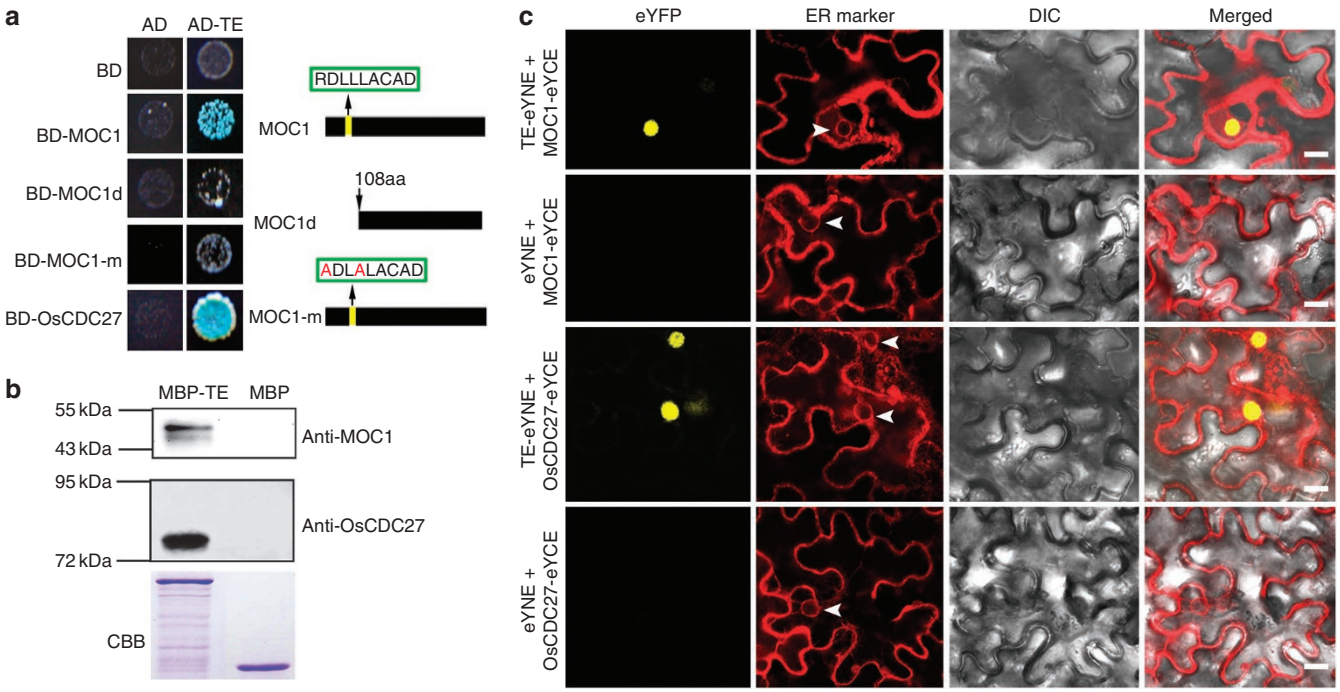

Figure 4 | TE physically interacts with MOC1 and OsCDC27. (**a**) Yeast two-hybrid assay showing that TE interacts with MOC1 and OsCDC27, but not with MOC1d and MOC1-m. The protein structure of MOC1 and MOC1d and the amino-acid substitutions in MOC1-m are shown on the right. (**b**) *In vitro* pull-down assay showing that MBP–TE, but not MBP itself, pulled down MOC1 (upper image) and OsCDC27 (middle image) from plant extracts. Coomassie blue staining (CBB) showing that roughly equal amounts of purified MBP-TE and MBP proteins were used in the pull-down assay (lower image). (**c**) BiFC assay showing that TE can interact with MOC1 and OsCDC27 in the nuclei of leaf cells of *N. benthamiana*. The signals of eYFP were not detected in the corresponding negative controls. White arrowheads indicate the nuclear membrane. Scale bar, 20 μm.

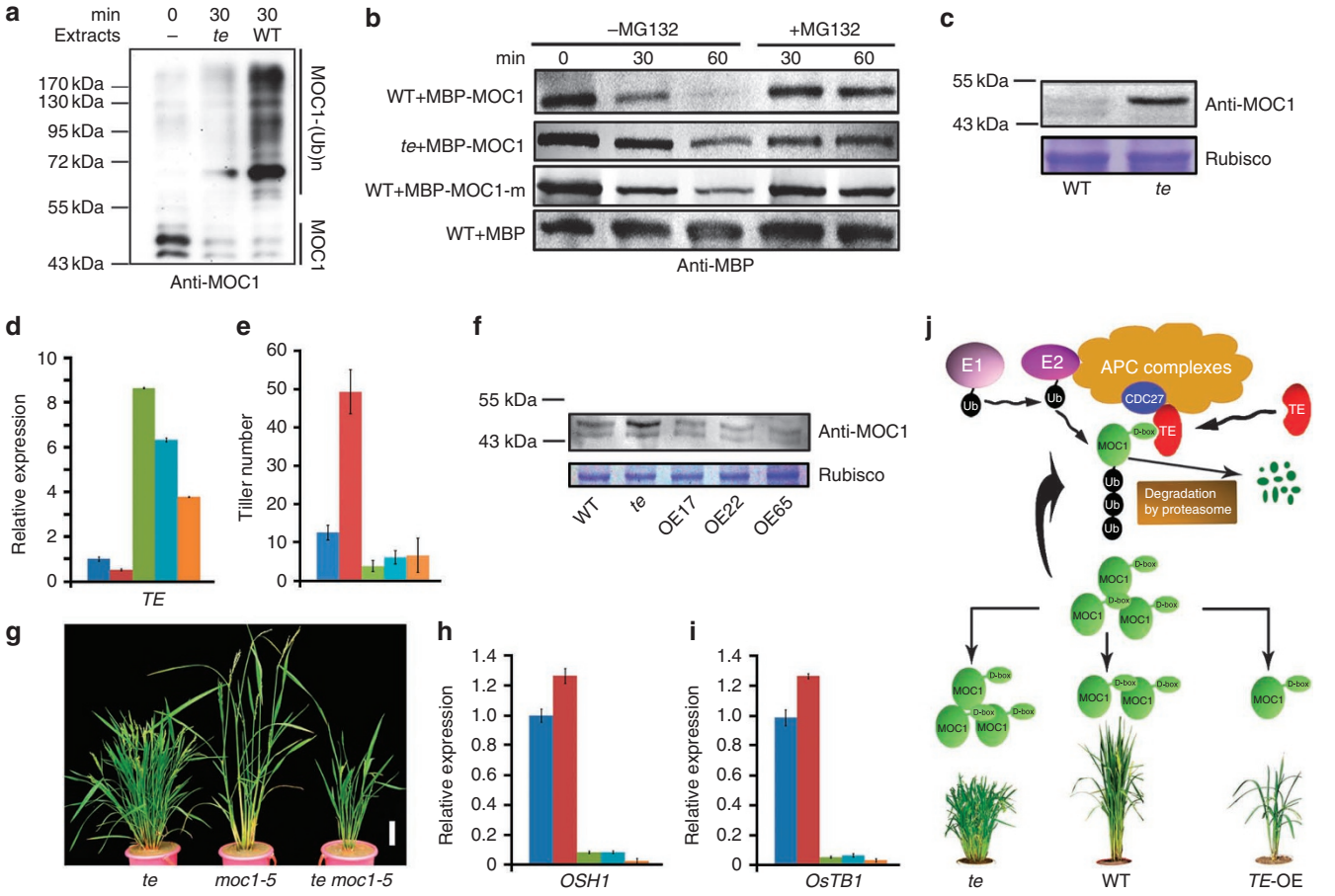

Figure 5 | TE mediates the degradation of MOC1 and it acts upstream of MOC1. (**a**) *In vitro* ubiquitination assay showing that MOC1 is ubiquitinated by WT plant extracts but not by *te* plant extracts. (**b**) Cell-free degradation assay showing that MBP-MOC1, but not MBP-MOC1-m and MBP, was degraded in WT plant extracts after 60 min incubation, whereas MBP-MOC1 remained relatively stable in *te* plant extracts. The degradation of MBP-MOC1 by plant extracts was blocked in the presence of 40 μM MG132 (+MG132). (**c**) Western blot analysis showing that MOC1 protein accumulated to a higher level in the *te* plants compared with WT (top). Rubisco strips showing a roughly equal loading of total proteins (bottom). (**d**) Quantitative RT–PCR assay showing that the expression level of *TE* is dramatically upregulated in OE17 (green), OE22 (light blue) and OE65 (orange), compared with WT (blue) or *te* (red). (**e**) OE17 (green), OE22 (light blue) and OE65 (orange) had reduced tiller numbers in comparison with WT (blue) or *te* (red). Data are mean±s.d. (n=15 plants). (**f**) Western blot analysis showing that there was less MOC1 protein in the *TE*-OE lines compared with WT and *te* (top). Rubisco strips showing the roughly equal loading of total proteins (bottom). (**g**) The *te moc1-5* double mutant have reduced tiller number as the *moc1-5* parent. Scale bar,10 cm. (**h**,**i**) Quantitative RT–PCR assay showing that the expression levels of *OSH1* and *OsTB1* were drastically reduced in OE17 (green), OE22 (light blue) and OE65 (orange) transgenic lines, but slightly increased in *te* (red) mutant, in comparison with WT (blue). (**j**) A model showing that TE activates the APC/C E3 ubiquitin ligase activity and targets MOC1 for degradation through interacting with the D-box, and consequently represses tillering. Error bars represent s.e.m. in **d**,**h**,**i** (n=3).

Methods

Plant materials. The *te* mutant was identified from the F_4 offsprings of pollen culture plants derived from the tetraploid hybrid H5409 (H2088xH3811)[26]. The normal offspring of pollen culture plants, with a nearly identical genetic background to *te*, was viewed as the wild type (WT) of *te* in this study. Genetic analysis showed that the twisted leaf phenotype of *te* is controlled by a single recessive nuclear locus, *TE*. To map the *TE* locus, we generated an F_2 mapping population derived from a cross between the *te* and the cultivar Zhenshan 97B.

Map-based cloning of *TE*. The *TE* locus was mapped to a 23-kb region between the simple sequence repeat marker RM523 and the InDel marker g62 on chromosome 3 using 1,800 F_2 mutant plants with additionally molecular markers developed in this work (Supplementary Table S1). The cDNA of the candidate gene, LOC_Os03g03150, was amplified from both *te* and WT using primers (Rt-1F 5′-ACCTTCCTCTCCTCTCCTCCC-3′ and Rt-1R 5′-TCAGTGTTTGCCATCTTCGCT-3′), and the PCR products were confirmed by sequencing.

Construction of *te moc1-5* double mutant. The *moc1-5* mutant was isolated from a population of *Nipponbare* treated by ^{60}Co-γ irradiation. The mutation locus was mapped with markers developed in this study (Supplementary Table S2). The *te moc1-5* double mutants were identified from F_2 offsprings of the hybrids between *te* and *moc1-5* mutant.

Complementation test and overexpression of *TE* in *te* plants. A 6.2-kb genomic DNA fragment (consisting of a 1.2-kb upstream sequence, the entire *TE* gene including ten exons and nine introns, and a 1.1-kb downstream region) was amplified using primers pGR-3F (5′-TGAATCTTACTCTTCTATATATTGCCTCAC-3′) and pGR-4R (5′-GGATCCCATAACCTTATTTATTTTTCTAGT-3′), and the PCR product was inserted into the binary vector pCAMBIA1305.1 to generate the transformation plasmid pGTE. The 1.8-kb cDNA sequence of *TE* was amplified using primers RT-2LF (5′-ATCCCCAAATCTCTCGCCCCCACCCA-3′) and RT-2LR (5′-TCGCTCCTACAAAGCCAATGAATAAA-3′), and the PCR fragment was inserted into the downstream of the ubiquitin promoter in the vector pCUBi 1390, resulting in plasmid pUBi::TE. The *te* was transformed with *Agrobacterium tumefaciens* strain EHA105 harbouring the plasmid pGTE or pUBi::TE.

RNA *in situ* hybridization. Shoot apexes of rice seedlings at the third and fourth leaf stages were fixed with an formalin acetic-acid alcohol (RNase-free) fixative solution at 4 °C overnight, followed by a series of dehydration steps and then embedded in paraffin (Paraplast Plus, Sigma). RNA *in situ* hybridization was performed as described previously[40]. The 5′ end of *TE* was amplified with primers pf2 (5′-ACTGAGATGTGGAGCGAAGATGG-3′) and pr2 (5′-TTGACATAGATCAGTACAAAGTTG-3′) and cloned into the pGEM-T Easy vector (Promega). Digoxigenin-labelled probes were prepared from linearized templates amplified from the pGEM-T plasmid containing the 5′ end of *TE* using primer Yt7 (5′-CCCA

GTCACGACGTTGTAAA-3′) and Ysp6 (5′-CACACAGGAAACAGCTATGAC-3′). Digoxigenin-labelled RNA probes were prepared using a DIG Northern Starter Kit (Cat. No. 2039672, Roche) following the instructions of manufacturer. The slides were observed under bright field with a microscope (Leica DM5000B) and photographed using a camera (Leica DFC490).

Subcellular localization. A 1,569-bp coding sequence of *TE* was amplified with the primer 52aXF (5′-CTAGATCTCGAGATGGATCACCACCACCACCACCTG-3′) and 52aSR (5′-CTAGACTAGTCGGATGTAGCTCCTAACAAATGATG-3′), and the PCR product was inserted into the *Xho*I/*Spe*I sites of the PA7 vector, to fuse to the upstream of GFP, resulting in the TE–GFP fusion protein-expressing plasmid PA7-TE, and then transformed into *Arabidopsis* protoplasts, as reported previously[41]. PA7 plasmid was used as the control.

Flow cytometry. About 30 flag leaves were chopped in 10 ml of a cold nuclear isolation buffer (10 mM $MgSO_4$, 50 mM KCl, 5 mM hepes (4-(2-hydroxyethyl) piperazine-1-ethanesulfonic acid), 3 mM dithiothreitol, pH 8.0. Triton X-100 at a final concentration of 0.25% before use). The crude extract with isolated cells was filtered (48 μm), then stained with 2.5 μg ml^{-1} 4′,6-diamidino-2-phenylindole (DAPI, Roche) and immediately analysed on an FACStar Plus cytometer (Becton Dickinson).

Overexpression of *TE* in *Schizosaccharomyces pombe*. The coding sequence of *TE* was amplified using primer 52aNF (5′-GGAATTCCATATGATGGATCACCAC CACCACCACCTG-3′) and 52aBR (5′-CTAGGAAGATCTTCACCGGATGTAG CTCCTAACAAATG-3′), and the PCR product was cloned into the pREP1 vector and verified by sequencing. In the absence of thiamine (-thiamine), overexpression of *TE* was induced in *S. pombe* as reported[3].

Construction of protein expression plasmids. *MOC1* and *TE* were amplified with the primers shown in Supplementary Table S3, and the PCR products were cloned into the pMAL-C2x vector (NEB), resulting in the plasmids pMAL-C2x::MBP-MOC1 and pMAL-C2x::MBP-Te. The D-box of MOC1 was mutated using a Phusion® Site-Directed Mutagenesis Kit (NEB) with the primers listed in Supplementary Table S3.

***In vitro* pull-down assay**. The seedlings of wild type were planted in the pots and grown in a climate chamber (HP1500GS, Ruihua) with a 14.5-h light (30 °C) – 9.5 h darkness (25 °C) photocycle. Total proteins were subsequently extracted in a degradation buffer[42]. The total protein concentration was determined by the Bio-Rad protein assay. For pull-down assay, roughly equal amounts of purified MBP and MBP–TE fusion proteins (about 1 μg) were affixed to Amylose Resin (NEB), and incubated in 400 μl of plant extract (containing 1.6 mg total proteins) in the presence of 42 μM MG132 gently shaken at 28 °C for 30 min. The pull-down analyses were performed as reported[43,44] and detected with anti-MOC1 or anti-OsCDC27 antibodies at 1:200 dilution. The horseradish peroxidase (HRP)-conjugated anti-rabbit IG (H + L) (1:5,000 dilution, MBL) was used as the second antibody. The western blots were developed with enhanced chemiluminescence (ECL) reagent (GE Healthcare).

Cell-free degradation assay. The total protein extracts were prepared as in the pull-down assay from *te* and WT seedlings, and were adjusted to equal concentration in the degradation buffer[42]. Then MG132 (Calbiochem) was selectively added to various *in vitro* degradation assays as indicated. For degradation of purified MBP, MBP-MOC1 and MBP-MOC1-m proteins, equal amounts of these purified proteins (about 500 ng) were incubated in 50 μl of rice total-protein extract (containing about 200 μg total proteins) at 28 °C for each assay. For mock controls, an equal amount of solvent for each drug was used. The extracts were incubated at 28 °C, and the samples were taken at the indicated intervals for determination of MBP, MBP-MOC1 and MBP-MOC1-m protein abundance by western blots with the HRP-conjugated Anti-MBP monoclonal antibody at 1:5,000 dilution (E8038L, NEB). The western blots were developed with ECL reagent (GE Healthcare).

Yeast two-hybrid assay. The coding sequences of *TE*, *OsCDC27*, *MOC1*, *MOC1d* and *MOC1-m* were amplified using gene-specific primers (Supplementary Table S4). *TE* was inserted into the pGADT7 vector (Clonetech), and *MOC1*, *MOC1d*, *MOC1-m* and *OsCDC27* were inserted into the pGBKT7 vector (Clonetech), respectively. The yeast two-hybrid assay was performed following the manufacturer's instructions.

Antibody preparation and western blot analysis. *MOC1* CDS was inserted into the pET32a vector. Purified His-MOC1 fusion protein was injected into rabbits to produce polyclonal antibodies of MOC1. Western blots were performed using antiserum against MOC1 and visualized by an enhanced HRP-DAB substrate kit (PA110, TIANGEN). For OsCDC27, the polypeptide FNQSSDSVPRRSAR was synthesized, and conjugated with keyhole limpet hemocyanin (KLH) to form KLH-FNQSSDSVPRRSAR. Subsequently, the conjugates were injected into rabbits to produce polyclonal antibodies against OsCDC27.

***In vitro* ubiquitination assay**. The purified MBP–MOC1 protein bound to the Amylose Resin (NEB) was incubated at 28 °C with equal amounts of rice seedling crude extract in a buffer containing 25 mM Tris–HCl pH 7.5, 10 mM $MgCl_2$, 5 mM dithiothreitol, 10 mM NaCl, 10 mM adenosine triphosphate and 40 μM MG132. After incubation at 28 °C for the intervals as indicated, the MBP–MOC1 and MBP–MOC1-(Ub)n fusion proteins were cleaved at room temperature by Factor Xa (NEB), following the manufacturer's instruction. The supernatant containing MOC1 or MOC1-(Ub)n was added with SDS–PAGE-loading buffer, then loaded on SDS–PAGE gel and western blots were performed using antibodies against MOC1 or antibodies against polyubiquitin (Beijing Protein Innovation, http://www.proteomics.org.cn/) at 1:200 dilution. The HRP-conjugated anti-rabbit IG (H + L) (1:5,000 dilution, MBL) was used as the second antibody. The western blots were developed with ECL reagent (GE Healthcare).

Quantitative RT–PCR analysis. RNA was extracted from frozen samples using the RNAprep Pure Plant Kit (Tiagen) following the manufacturer's instructions. Quantitative RT–PCRs were performed by a SYBR Premix Ex Taq™ RT–PCR kit (Takara) following the manufacturer's instructions with the primers listed in Supplementary Table S5.

BiFC assay. CDS of *TE* was amplified with primer 52aSF (5′-GGAATTCACTAG TATGGATCACCACCACCACCACCTG-3′) and 52aKR (5′-CTAGGAGGTAC CCCGGATGTAGCTCCTAACAAATG-3′), then cloned into the *Spe*I/*Kpn*I sites of the vector pSPYNE173 (eYNE)[45] to form the TE-eYNE plasmid. CDS of *MOC1* was amplified with primer MOC1BF (5′-AGATTCGGATCCATGCTC CGGTCACTCCACTCCTC-3′) and MOC1KR (5′-CTAGGAGGTACCCGAC GACGACGGCTGC-3′), then cloned into the Bam HI/Kpn I sites of the vector pSPYCE(M) (eYCE)[45] to form the MOC1-eYCE plasmid. CDS of *OsCDC27* was amplified with primer CDC27SF (5′-GGAATTCACTAGTATGGAAACCCTAAT GGTGGACCG-3′) and CDC27XR (5′-CTAGGACTCGAGAATCTCATCAT CATCATCATCATCATCC-3′), then cloned into the *Spe*I/*Xho*I sites of the vector pSPYCE(M) to form the CDC27-eYCE plasmid.

For transient expression, *A. tumefaciens* strain AH109 carrying the BiFC constructs were used together with the p19 strain[46] and ER marker, mCherry ER-rk CD3-959[47], for infiltration of 5–6-week-old *N. benthamiana* leaves, as described in Waadt and Kudla[48]. Infiltrated leaves were observed 48–72 h after infiltration using a laser confocal scanning microscope (ZEISS Microsystems LSM 700, http://www.zeiss.com.cn/microscopy). The eYFP and mCherry fluorescent signals from the expressed fusion constructs were monitored sequentially. The excitation and detection wavelengths for eYFP and mCherry were 514 and 587 nm for excitation, and 527 and 610 nm for detection, respectively.

References

1. Peters, J. The anaphase promoting complex/cyclosome: a machine designed to destroy. *Nat. Rev. Mol. Cell Biol.* **7,** 644–656 (2006).
2. Li, M. & Zhang, P. The function of APC/C^{Cdh1} in cell cycle and beyond. *Cell Div.* **4,** 2 (2009).
3. Tarayre, S., Vinardell, J. M., Cebolla, A., Kondorosi, A. & Kondorosi, E. Two classes of the Cdh1-type activators of the anaphase-promoting complex in plants: novel functional domains and distinct regulation. *Plant Cell* **16,** 422–434 (2004).
4. Cebolla, A. *et al.* The mitotic inhibitor *ccs52* is required for endoreduplication and ploidy-dependent cell enlargement in plants. *EMBO. J.* **18,** 4476–4484 (1999).
5. Schaeffer, V., Althauser, C., Shcherbata, H. R., Deng, W. M. & Ruohola-Baker, H. Notch-dependent Fizzy-related/Hec1/Cdh1 expression is required for the mitotic-to-endocycle transition in *Drosophila* follicle cells. *Curr. Biol.* **14,** 630–636 (2004).
6. Narbonne-Reveau, K. *et al.* APC/$C^{Fzr/Cdh1}$ promotes cell cycle progression during the *Drosophila* endocycle. *Development* **135,** 1451–1461 (2008).
7. Da, F. P. *et al.* Structures of APC/$C^{(Cdh1)}$ with substrates identify Cdh1 and Apc10 as the D-box co-receptor. *Nature* **470,** 274–278 (2011).
8. Vanstraelen, M. *et al.* APC/C^{CCS52A} complexes control meristem maintenance in the *Arabidopsis* root. *Proc. Natl Acad. Sci. USA* **106,** 11806–11811 (2009).
9. Lammens, T. *et al.* Atypical E2F activity restrains APC/$C^{CCS52A2}$ function obligatory for endocycle onset. *Proc. Natl Acad. Sci. USA* **105,** 14721–14726 (2008).
10. Larson-Rabin, Z., Li, Z., Masson, P. H. & Day, C. D. *FZR2/CCS52A1* expression is a determinant of endoreduplication and cell expansion in Arabidopsis. *Plant Physiol.* **149,** 874–884 (2009).
11. Kasili, R. *et al.* SIAMESE cooperates with the CDH1-like protein CCS52A1 to establish endoreplication in *Arabidopsis thaliana* trichomes. *Genetics* **185,** 257–268 (2010).
12. Mathieu-Rivet, E. *et al.* Functional analysis of the anaphase promoting complex activator CCS52A highlights the crucial role of endo-reduplication for fruit growth in tomato. *Plant J.* **62,** 727–741 (2010).
13. Wang, Y. & Li, J. Molecular basis of plant architecture. *Annu. Rev. Plant Biol.* **59,** 253–279 (2008).
14. Xing, Y. & Zhang, Q. Genetic and molecular bases of rice yield. *Annu. Rev. Plant Biol.* **61,** 421–442 (2010).

15. Schumacher, K., Schmitt, T., Rossberg, M., Schmitz, G. & Theres, K. The *Lateral suppressor* (*Ls*) gene of tomato encodes a new member of the VHIID protein family. *Proc. Natl Acad. Sci. USA* **96,** 290–295 (1999).
16. Greb, T. *et al.* Molecular analysis of the *LATERAL SUPPRESSOR* gene in *Arabidopsis* reveals a conserved control mechanism for axillary meristem formation. *Genes Dev.* **17,** 1175–1187 (2003).
17. Li, X. *et al.* Control of tillering in rice. *Nature* **422,** 618–621 (2003).
18. Komatsu, K. *et al. LAX* and *SPA*: Major regulators of shoot branching in rice. *Proc. Natl Acad. Sci. USA* **100,** 11765–11770 (2003).
19. Gallavotti, A. *et al.* The role of *barren stalk1* in the architecture of maize. *Nature* **432,** 630–635 (2004).
20. Gomez-Roldan, V. *et al.* Strigolactone inhibition of shoot branching. *Nature* **455,** 189–194 (2008).
21. Tabuchi, H. *et al. LAX PANICLE2* of rice encodes a novel nuclear protein and regulates the formation of axillary meristems. *Plant Cell* **23,** 3276–3287 (2011).
22. Long, J. A., Moan, E. I., Medford, J. I. & Barton, M. K. A member of the KNOTTED class of homeodomain proteins encoded by the *STM* gene of Arabidopsis. *Nature* **379,** 66–69 (1996).
23. Vollbrecht, E., Veit, B., Sinha, N. & Hake, S. The developmental gene *Knotted-1* is a member of a maize homeobox gene family. *Nature* **350,** 241–243 (1991).
24. Matsuoka, M. *et al.* Expression of a rice homeobox gene causes altered morphology of transgenic plants. *Plant Cell* **5,** 1039–1048 (1993).
25. Khush, G. Productivity improvements in rice. *Nutr. Rev.* **61,** S114–S116 (2003).
26. Qin, R., Cheng, Z. & Guo, X. The establishment of mutant pool using anther culture of autotetrapolyploid rice. *ACTA AGRONOMICA SINICA* **31,** 392–394 (2005).
27. Garci-Higuera, I. *et al.* Genomic stability and tumour suppression by the APC/C cofactor Cdh1. *Nat. Cell Biol.* **10,** 802–811 (2008).
28. Wasch, R., Robbins, J. A. & Cross, F. R. The emerging role of APC/C^{Cdh1} in controlling differentiation, genomic stability and tumor suppression. *Oncogene* **29,** 1–10 (2010).
29. Kano-Murakami, Y., Yanai, T., Tagiri, A. & Matsuoka, M. A rice homeotic gene, *OSH1*, causes unusual phenotypes in transgenic tobacco. *FEBS Lett.* **334,** 365–368 (1993).
30. Sato, Y. *et al.* A rice homeobox gene, *OSH1*, is expressed before organ differentiation in a specific region during early embryogenesis. *Proc. Natl Acad. Sci. USA* **93,** 8117–8122 (1996).
31. Takeda, T. *et al.* The *OsTB1* gene negatively regulates lateral branching in rice. *Plant J.* **33,** 513–520 (2003).
32. Doebley, J., Stec, A. & Hubbard, L. The evolution of apical dominance in maize. *Nature* **386,** 485–488 (1997).
33. Otsuga, D., DeGuzman, B., Prigge, M. J., Drews, G. N. & Clark, S. E. *REVOLUTA* regulates meristem initiation at lateral positions. *Plant J.* **25,** 223–236 (2001).
34. Keller, T., Abbott, J., Moritz, T. & Doerner, P. Arabidopsis *REGULATOR OF AXILLARY MERISTEMS1* controls a leaf Axil stem cell niche and modulates vegetative development. *Plant Cell* **18,** 598–611 (2006).
35. Schmitz, G. *et al.* The tomato *Blind* gene encodes a MYB transcription factor that controls the formation of lateral meristems. *Proc. Natl Acad. Sci. USA* **99,** 1064–1069 (2002).
36. Oikawa, T. & Kyozuka, J. Two-step regulation of LAX PANICLE1 protein accumulation in axillary meristem formation in rice. *Plant Cell* **21,** 1095–1108 (2009).
37. Vinardell, J. M. *et al.* Endoreduplication mediated by the anaphase-promoting complex activator CCS52A Is required for symbiotic cell differentiation in *Medicago truncatula* nodules. *Plant Cell* **15,** 2093–2105 (2003).
38. Hu, D., Qiao, X., Wu, G. & Wan, Y. The emerging role of APC/C^{Cdh1} in development. *Semin. Cell Dev. Biol.* **22,** 579–585 (2011).
39. Beveridge, C. A. & Kyozuka, J. New genes in the strigolactone-related shoot branching pathway. *Curr. Opin. Plant Biol.* **13,** 34–39 (2010).
40. Bradley, D., Carpenter, R., Sommer, H., Hartley, N. & Coen, E. Complementary floral homeotic phenotypes result from opposite orientations of a transposon at the *plena* locus of Antirrhinum. *Cell* **72,** 85–95 (1993).
41. Sheen, J. A transient expression assay using *Arabidopsis* mesophyll protoplasts, http://genetics.mgh.harvard.edu/sheenweb/ (2002).
42. Wang, F. *et al.* Biochemical insights on degradation of *Arabidopsis* DELLA proteins gained from a cell-free assay system. *Plant Cell* **21,** 2378–2390 (2009).
43. Miernyk, J. A. & Thelen, J. J. Biochemical approaches for discovering protein-protein interactions. *Plant J.* **53,** 597–609 (2008).
44. Tagwerker, C. *et al.* A tandem affinity tag for two-step purification under fully denaturing conditions: application in ubiquitin profiling and protein complex identification combined with *in vivo* cross-linking. *Mol. Cell Proteomics* **5,** 737–748 (2006).
45. Waadt, R. *et al.* Multicolor bimolecular fluorescence complementation reveals simultaneous formation of alternative CBL/CIPK complexes in planta. *Plant J.* **56,** 505–516 (2008).
46. Voinnet, O., Rivas, S., Mestre, P. & Baulcombe, D. An enhanced transient expression system in plants based on suppression of gene silencing by the p19 protein of tomato bushy stunt virus. *Plant J.* **33,** 949–956 (2003).
47. Nelson, B. K., Cai, X. & Nebenfuhr, A. A multicolored set of *in vivo* organelle markers for co-localization studies in Arabidopsis and other plants. *Plant J.* **51,** 1126–1136 (2007).
48. Waadt, R. & Kudla, J. In Planta Visualization of Protein Interactions Using Bimolecular Fluorescence Complementation (BiFC). *Cold Spring Harbor Protocols* **2008,** t4995 (2008).

Acknowledgements

This work was supported by 973 National Basic Research Program of China (2010CB125904-4), National Natural Science Foundation (Grant 31000667), 863 National High-tech R&D Program of China (2012AA100101) and Ministry of Agriculture of the People's Republic of China. We thank Dr. Lilin Du of NIBS for providing the yeast vector pREP1, Dr. Hongquan Yang (Shanghai Jiaotong University, China) for the gift of plasmid PA7-GFP and Dr. Mao-Yun She (Institute of Crop Science, Chinese Academy of Agricultural Sciences, Beijing) for technical assistance with flow cytometry assay. We thank Dr. Zhenbiao Yang (UC-Riverside), Dr. Roger Pennell (Ceres, Inc.) and Dr. Chentao Lin (UC-Los Angeles) for critical reading and comments on the manuscript.

Author contributions

J.W. and H.W. supervised the project. Z.C., J.G., R.Q. and J.L.W. identified the *te* mutant and performed genetic analysis and mapping of *TE*. Q.L., D.W., H.D. and S.G. performed other experiments and data analysis. J.W., Q.L. and H.W. wrote the manuscript.

Additional information

Supplementary Information accompanies this paper at http://www.nature.com/naturecommunications

Competing financial interests: The authors declare no competing financial interests.

Reprints and permission information is available online at http://npg.nature.com/reprintsandpermissions/

How to cite this article: Lin, Q. *et al.* Rice APC/C^{TE} controls tillering by mediating the degradation of MONOCULM 1. *Nat. Commun.* 3:752 doi: 10.1038/ncomms1716 (2012).